Journal of Nuclear Medicine, published on May 8, 2020 as doi:10.2967/jnumed.120.246983

The effects of monosodium glutamate on PSMA radiotracer uptake in men with recurrent prostate cancer: a prospective, randomized, double-blind, placebo-controlled intra-individual imaging study

Authors: Sara Harsini[1], Heather Saprunoff[1], Tina Alden[1], Behnoud Mohammadi[1], Don Wilson[1] and François Bénard[1,2].

[1]BC Cancer, 600 West 10th Avenue, Vancouver, BC, V5Z 4E6
[2]Department of Radiology, University of British Columbia, 2775 Laurel St., Vancouver, BC Canada V5Z 1M9

Corresponding Author:
François Bénard, MD, FRCPC
675 West 10th Ave
Vancouver BC, Canada
Email: fbenard@bccrc.ca
Phone: 1-604-675-8206
Fax: 1-604-675-8218

First Author:
Sara Harsini, MD, MPH (Resident)
675 West 10th Ave
Vancouver BC, Canada
Email : sharsini@bccrc.ca
Phone: 1-604-675-8000

Running Title: MSG and PSMA radiotracer uptake

Word Count: 5403

Financial Support: This study was carried out with the financial support of the BC Cancer Foundation, CIHR grant FDN #FDN-148465 and the BC Leadership Chair in Functional Cancer Imaging.

Abstract

The prostate-specific membrane antigen (PSMA) is an excellent target for theranostic applications in prostate cancer (PCa). However, PSMA-targeted radioligand therapy can cause undesirable effects due to high accumulation of PSMA radiotracers in salivary glands and kidneys. This study assessed orally administered monosodium glutamate (MSG) as a potential means of reducing kidney and salivary gland radiation exposure using a PSMA targeting radiotracer.

Methods: This prospective, double-blind, placebo-controlled study enrolled 10 biochemically recurrent PCa patients. Each subject served as his own control. [^{18}F]DCFPyl PET/CT imaging sessions were performed 3 – 7 days apart, following oral administration of either 12.7 g of MSG or placebo. Data from the two sets of images were analyzed by placing regions of interest on lacrimal, parotid and submandibular glands, left ventricle, liver, spleen, kidneys, bowel, urinary bladder, gluteus muscle and malignant lesions. The results from MSG and placebo scans were compared by paired analysis of the ROI data.

Results: A total of 142 pathological lesions along with normal tissues were analyzed. As hypothesized a priori, there was a significant decrease in maximal standardized uptake values corrected for lean body mass (SULmax) on images obtained following MSG administration in the parotids (24 ± 14%, P=0.001), submandibular glands (35 ± 11%, P<0.001) and kidneys (23 ± 26%, P=0.014). Significant decreases were also observed in lacrimal glands (49 ± 13%, P<0.001), liver (15 ± 6%, P<0.001), spleen (28 ± 13%, P=0.001) and bowel (44 ± 13%, P<0.001). Mildly lower blood pool SULmean was observed after MSG administration (decrease of 11 ± 13%, P=0.021). However, significantly lower radiotracer uptake in terms of SULmean, SULpeak, and SULmax was observed in malignant lesions on scans performed after MSG administration compared to the

placebo studies (SULmax median decrease 33%, range -1 to 75%, P<0.001). No significant adverse events occurred and vital signs were stable following placebo or MSG administration.

Conclusion: Orally administered MSG significantly decreased salivary gland, kidney and other normal organ PSMA radiotracer uptake in human subjects, using [^{18}F]DCFPyL as an exemplar. However, MSG caused a corresponding reduction in tumor uptake, which may limit the benefits of this approach for diagnostic and therapeutic applications.

Key words: *Monosodium glutamate; PSMA; prostate-specific membrane antigen; salivary glands; kidney*

Introduction

Prostate cancer (PCa) is the principal cause of cancer mortality in men worldwide due to the development of metastatic disease *(1)*. Advanced stages of PCa initially respond to androgen deprivation therapy (ADT), but within an interval of one to three years, they invariably develop androgen independence *(2)*. Other therapeutic agents approved for the treatment of metastatic castration-resistant PCa (mCRPC) (cabazitaxel *(3)*, abiraterone *(4)*, sipuleucel-T *(5)*, enzalutamide *(6)*, and radium-223 *(7)*) can improve survival. However, none culminated in durable clinical responses, with a survival benefit of generally less than 6 months *(6)*. The prostate-specific membrane antigen (PSMA), a type II, carboxypeptidase-associated transmembrane glycoprotein with folate hydrolase activity, is overexpressed in PCa cells *(8)*. Several radiolabeled PSMA ligands, showing high sensitivity or specificity for PSMA-expressing tissues, have been investigated in positron emission tomography (PET) imaging *(9)*. Current evidence suggests that PSMA-targeting radioligand therapy (RLT) shows promise to treat mCRPC patients, by employing ligands such as β-emitting (lutetium-177) or α-emitting isotopes (actinium-225) *(10, 11)*.

One of the major disadvantages of PSMA-RLT is the high accumulation of the radiolabeled tracers in non-target organs, including the salivary glands and kidneys. High accumulation of the PSMA radiopharmaceuticals in salivary glands can result in transient or permanent xerostomia, an adverse event with a variable reported rate of 8–87%, which is particularly problematic with ^{225}Ac, leading to treatment discontinuation in many cases *(10, 12)*. On the other hand, renal accumulation of beta emitters such as [^{177}Lu]Lu-PSMA-617 represents the cumulative dose-limiting toxicity and leads to risk of nephrotoxicity *(13)*. Furthermore, the increased risk of chronic renal disease prevents initiation of PSMA-RLT earlier in disease course *(14)*. Many attempts including sialendoscopy

with dilatation, saline irrigation, steroid injection, intraparenchymal injections of botulinum toxin, external cooling of the salivary glands with ice-packs and oral administration of folic polyglutamate tablets have been tried to mitigate salivary gland toxicity with some, but limited success *(15-18)*. Mannitol infusion is a strategy to reduce renal uptake of PSMA-targeted tracers by acting as an osmotic diuretic, decreasing renal reabsorption. However, its effect on tumor uptake needs to be clarified *(19)*. The administration of 2-(phosphonomethyl)pentane-1,5-dioic acid (2-PMPA), a phosphonate-based PSMA inhibitor, reduced accumulation of PSMA radiotracers in the kidneys in a dose-dependent manner, but this was generally accompanied by decreased tumor uptake *(20-22)*. A novel 2-PMPA prodrug (e.g., Tris-POC-2-PMPA) has been proposed to specifically shield the kidneys and salivary glands from PSMA-RLT, however, its effect on tumor uptake requires further studies *(23)*. We recently reported that the administration of monosodium glutamate (MSG), a well-known food additive, reduced salivary and kidney [^{68}Ga]Ga-PSMA-11 uptake in LNCap tumor-bearing mice, while tumor uptake remained unaffected *(24)*.

In this study we explored the effects of MSG in human subjects on the biodistribution of a PSMA targeting radiopharmaceutical. We performed an intra-individual comparison of the biodistribution of [^{18}F]DCFPyL in patients with biochemical recurrence of PCa, comparing scans performed with the prior administration of orally administered MSG or placebo. We evaluated the uptake of [^{18}F]DCFPyL in normal organs and malignant lesions to determine whether MSG could be reduce-off target binding of PSMA targeting radiopharmaceuticals as a potential strategy to improve the therapeutic ratio of RLT.

Materials and Methods

Patients

The study included 10 patients with any of the following criteria: (1) known prostate cancer with biochemical recurrence after initial curative radiation therapy, with a PSA level > 2 ng/mL above the nadir after therapy; and (2) known prostate cancer with biochemical recurrence after initial curative radical prostatectomy, with a PSA > 0.4 ng/mL and an additional measurement showing increase. Exclusion criteria were: (1) medical instability; (2) inability to lie supine for imaging; (3) inability to provide written consent; (4) exceeding the safe weight of the positron emission tomography/computed tomography (PET/CT) bed (204.5 kg) or inability to fit through the PET/CT bore (70 cm diameter); (5) ECOG > 2; (6) severe uncontrolled hypertension; (7) history of severe asthma; (8) history of intolerance to MSG; (9) history of severe headaches or migraines triggered by food or MSG; and (10) being on a sodium/salt restricted diet due to other medical conditions. Although no treatment was discontinued before the [^{18}F]DCFPyL scan, no new treatment was initiated between the first and second [^{18}F]DCFPyL PET/CT. The patients were randomly assigned to receive either placebo or MSG prior to the first PET acquisition, then crossed over to the other intervention for a repeat scan within 3-7 days. The patients, research staff acquiring the studies and scan readers were blinded to as to whether the subjects received placebo or MSG.

The study was approved by the UBC/BC Cancer Research Ethics Board and by Health Canada. Written informed consent was provided by all participants prior to inclusion in the study. The study was registered on ClinicalTrials.gov (Identifier: NCT03693742).

Study Procedures

Patient demographics, relevant oncological history, laboratory values and tumor pathology data were recorded. Participants were followed-up 24h after radiotracer administration to identify adverse events.

[^{18}F]DCFPyL was synthesized according to a previously published method *(25)*. The administered activity was scaled by body weight (range: 237-474 MBq), allowing a 10% variation in target activity. After a 4-hour fast and 30 minutes prior to [^{18}F]DCFPyL intravenous injection, each participant ingested either 300 mL ± 5% of low sodium tomato juice (Heinz) containing 12.7 g MSG, or regular tomato juice (Heinz; placebo), according to a computer generated random list which determined the sequence of the scans. Second PET/CT examinations were performed within an interval of 3-7 days.

Vital signs were recorded before administration of MSG, before [^{18}F]DCFPyL injection, between 5 to 15 minutes after [^{18}F]DCFPyL injection, and 60 minutes after radiotracer injection. Between 60 and 120 minutes, participants were allowed to have a meal of their choice. After a 120-minute uptake period, vital signs were monitored again, and the participants were imaged from top-of-head to mid-thigh on a Discovery PET/CT 690 (GE Healthcare). A CT scan for localization and attenuation correction (120 kV, automatic mA selection (30-200 mA range) and noise index of 20) was acquired. PET data were acquired immediately after the CT over 2-4 minutes/bed position, adjusted for participant girth. All images were reconstructed identically using the ordered subset expectation maximization algorithm and point-spread function modeling.

Image Interpretation

Two nuclear medicine physicians with access to all clinical data reviewed the PET/CT images reconstructed without the time-of-flight option using a MIM workstation (MIM Encore™ version

6.9.4, MIM Software Inc.). PET, CT, and fused PET/CT images were reviewed in axial, coronal, and sagittal planes in two reading sessions. The readers were blinded as to which intervention occurred prior to the scan they were interpreting (MSG/control). After visual qualitative identification of the tumoral lesions, a semiquantitative evaluation was performed on the basis of standardized uptake value (SUV) adjusted for the lean body mass (SUL), reflecting a maximum single-pixel uptake value, the peak SUL (SULpeak), calculated using an automated computed maximal average SUL in a 1.0 cm^3 spherical volume within the tumor, and mean SUL (SULmean). For normal organs, regions of interest (ROIs) were drawn at predetermined reference sites including the lacrimal, parotid and submandibular glands, left ventricle blood pool, liver, spleen, kidneys, bowel, urinary bladder, and gluteus muscle. The arithmetic mean was calculated for paired organs. For all malignant lesions, the SULmax, SULmean, and SULpeak were measured using the PET Edge tool running on MIM. All ROIs were created in one dataset by a blinded observer, and then saved and compared to the identical location in the second dataset for matched comparisons of activity.

Statistical Analysis

Descriptive values were expressed as the mean (± SD) or median [range] if data were not normally distributed according to the Shapiro-Wilk test. The relative percentages of SULmax, SULmean, and SULpeak change between control and MSG studies were calculated as: [(MSG (value) – Control (value))/Control (value)] × 100. Independent Student's t-test was performed to compare normal variables, otherwise, non-parametric tests including Wilcoxon's signed-rank test for paired data was used to compare malignant lesions SULmean, SULmax and SULpeak. To adjust for multiple testing and control the false discovery rate (FDR), the Benjamini–Hochberg method was

used *(26)*. Finally, the sample was adjusted by a weight factor, using the *Weight Cases* option in the SPSS software in malignant lesions' analysis, in order to balance the sample in accordance with the uneven frequency of malignant lesions in different patients. The correlation of percentages of SULmax change between control and MSG studies (for salivary glands and kidneys) with MSG doses was compared by Pearson correlation test. To examine changes in vital signs over the study period, an ANOVA for repeated measures was used. Statistical analyses were conducted using the IBM SPSS Statistics 25.0 (IBM corporation. Armonk, NY, USA) and R (version 3.6.0; The R Foundation for Statistical Computing, General Public License). A P value of less than 0.05 was considered significant.

Results

Demographic Characteristics

As depicted in Table 1, this prospective analysis included 10 patients (mean age 72 ± 4.5 years) of whom 6 had a biochemical recurrence after radical prostatectomy and 4 had a biochemical recurrence after curative intent radiotherapy. Prior treatments included surgery (60% of cases), radiotherapy (90%) or androgen deprivation therapy (ADT) (30%), with 60% of participants having received more than one type of therapy. Overall, the subjects had a mean PSA of 6.62 ± 9.56 ng/mL with a doubling time of 11.3 ± 12.2 (n=9) months. Representative MSG and control [^{18}F]DCFPyL PET/CT scans are shown in Fig. 1.

Normal Tissues

The average SULmean and SULmax values of different normal tissues in all patients for both MSG and control PET/CTs are described in Table 2. Statistically significant lower SULmean after MSG administration compared to the placebo group were noted in the left ventricle blood pool

(10.72 ± 12.54%, P=0.03), liver (15.75 ± 7.32%, P<0.001), spleen (34.34 ± 11.11%, P<0.001), parotid glands (26.07 ± 16.98%, P=0.004), submandibular glands (34.68 ± 18.68%, P=0.001), lacrimal glands (41.88 ± 18.88%, P<0.001), bowel (45.08 ± 13.83%, P<0.001) and kidneys (27.39 ± 12.07%, P=0.001). The SULmean was lower in the gluteus muscle (7.92 ± 21.72%, P=0.17) and urinary bladder (14.85 ± 30.22%, P=0.08) but this did not reach statistical significance.

In addition, the SULmax was significantly lower in the liver (14.60 ± 5.75%, P<0.001), spleen (28.27 ± 13.39%, P=0.001), parotid glands (23.98 ± 14.03%, P=0.001), submandibular glands (35.03 ± 11.19%, P<0.001), lacrimal glands (48.53 ± 12.54%, P<0.001), bowel (43.77 ± 12.95%, P<0.001) and kidneys (23.46 ± 26.08%, P=0.014). Lower SULmax in the left ventricle blood pool (11.42 ± 19.08%, P=0.11), gluteus muscle (2.67 ± 27.96%, P=0.61) and urinary bladder (14.45 ± 32.49%, P=0.19) did not reach statistical significance.

The most reproducible trend was seen in the parotid, submandibular and lacrimal glands, liver, spleen and bowel, with all patients demonstrating lower SULmean and SULmax on PET/CT images following MSG administration compared to the control group. The comparison between MSG and control SULmax values is shown in Fig. 2.

When the MSG amount was normalized to body weight, no significant dose-response relationship could be demonstrated for percentage changes of salivary gland and renal SULmax (supplemental Fig. 1).

Malignant Lesions

At least one lesion characteristic of PCa was detected in each patient. Active disease was most often characterized in lymph nodes (67.6%), followed by bone (29.6%) and prostate bed/seminal vesicles (2.8%). Seven participants (70%) had disease in more than one site. Overall, 142 lesions

were detected on both MSG and control images with significantly higher median SULpeak in the control compared to the MSG group 4.13 vs 3.01 (P<0.001), median SULmean 2.88 vs 1.57 (P<0.001) and median SULmax 4.36 vs 2.78 (P<0.001), for the control and MSG groups, respectively (Table 3). The decrease was significant for local recurrences, lymph nodes and osseous metastases (Fig. 3). All lesions were visible on both MSG and control images, with the exception of two osseous metastases that were visible on control images only.

Adverse Events

Vital signs at different time-points are as follows in the MSG group: blood pressure changed from 156.80 ± 12.03/92.20 ± 8.57 to 154.90 ± 15.63/84.10 ± 7.63 mmHg between pre-MSG values and immediately before the scan. The heart rate changed from 71.70 ± 10.67 to 86.70 ± 12.31 bpm, and pulse oximetry from 97.90 ± 1.66 to 97.20 ± 1.87%. In the placebo group, blood pressure changed from 153.40 ± 18.66/90.60 ± 6.62 to 151.80 ± 17.54/85.70 ± 7.21 mmHg between pre-placebo values and two hours after the radiotracer injection. The heart rate changed from 68.40 ± 7.95 to 74.20 ± 11.07 bpm, and pulse oximetry from 98.20 ± 1.75 to 97.90 ± 1.52%. Except for heart rate in the MSG group, these values were not statistically significant. Heart rate alterations were considered clinically insignificant. There were no adverse events during scans.

Discussion

PSMA-targeting radioligand therapy is a promising treatment with a significant impact on prostate cancer management *(27-29)*. ^{177}Lu- and ^{225}Ac-labeled PSMA ligands have shown efficacy in mCRPC patients, but physiological tracer uptake in salivary glands and kidneys can cause xerostomia and potential for nephrotoxicity *(30, 31)*. The fact that radiolabeled anti-PSMA antibodies have low uptake in these organs supports the hypothesis that beyond PSMA expression,

the accumulation of small-molecule PSMA inhibitors could be partially attributed to off-target binding *(32, 33)*. Although this undesired uptake of PSMA ligands in normal PSMA expressing organs does not hinder diagnostic interpretation, it imposes a limit on the maximum tolerable dose for PSMA-RLT. Notwithstanding the fact that xerostomia typically appears after the second or third cycles of PSMA-RLT, discontinuation of this mode of therapy has been reported in patients treated with alpha emitters *(34)*. Late stage, heavily pre-treated mCRPC patients with resistant disease constitute the main category of patients in whom these treatments have thus far been offered. The poor life expectancy of this group likely masks the emergence of late radiation-induced kidney failure, which generally requires 2 or more years to manifest *(35)*. However, renal toxicity might become a more significant concern if PSMA-RLT were to be initiated in patients at an early stage of (high risk) PCa with (oligo)-metastatic disease *(36)*. A protection approach to meaningfully mitigate toxicities associated with PSMA radiotherapeutics would be useful to enable the broadest, earliest and most effective use of these radiotherapeutics.

A few investigations have suggested protective approaches to mitigate PSMA radioligand accumulation in these organs. Rousseau *et al. (24)* reported that intraperitoneal injection of up to 164 mg/kg MSG in LNCap tumor bearing NOD SCID gamma (NSG) mice resulted in lower salivary and kidney uptake of [^{68}Ga]Ga-PSMA-11 in a dose-dependent manner, whereas tumor uptake was unaffected. Considering the fact that the majority of PSMA ligands integrate a glutamate moiety to bind to PSMA, it was postulated that the administration of MSG could act by blocking non-specific binding in healthy organs *(24)*.

Hillier *et al.* showed near complete blockade of tumor and kidney uptake of the PSMA inhibitor [^{123}I]MIP-1095 following coinjection of 2-PMPA *(37)*. The potential of 2-PMPA to selectively block kidney uptake without affecting LNCaP tumor uptake was demonstrated by Kratochwil *et*

al. through administration of 2-PMPA 1 or 16 hours after injection of the PSMA inhibitors [^{99m}Tc]Tc-MIP-1404 and [^{125}I]MIP-1095, respectively *(22)*. Chatalic *et al.* showed improved tumor-to-kidney absorbed dose ratio by coinjection of 2-PMPA with [^{111}In/^{177}Lu]In/Lu-PSMA I&T, which was accompanied by a reduction in tumor uptake *(21)*.

Among recently developed orally available prodrugs of 2-PMPA *(23)*, JHU-2545 has been administered in a small number of mCRPC patients 15 minutes prior to injection of [^{177}Lu]Lu-PSMA-617 and was found to lead to increase the metastases and/or salivary gland dose ratio to 350%-550% of control values, and the metastases and/or kidney dose ratio to between 190% and 650% of control. Based on the available dosimetry, Nedelcovych *et al.* concluded that this prodrug could increase the cumulative allowable [^{177}Lu]Lu-PSMA-617 dose by two to six-fold *(38)*.

Supported by favorable preclinical data obtained with [^{68}Ga]Ga-PSMA-11, the present study aimed to assess orally administered MSG as a potential means of reducing normal organ PSMA-targeting radiotracer uptake in human subjects. We observed a significant decrease in SULmax on images obtained following MSG administration in the parotids, submandibular glands, kidneys, lacrimal glands, liver, spleen and bowel. Mildly lower blood pool SULmean was also observed after MSG administration. Hence, our results indicated that the uptake of [^{18}F]DCFPyL in normal tissues was blocked by the administration of MSG, with the highest effect being noted in the lacrimal glands, followed by colon. However, lower radiotracer uptake was unfortunately observed in malignant lesions on scans performed after MSG administration compared to the placebo studies.

The findings of this study were in line with our previously reported preclinical results, except for the decrease in malignant prostate lesions, which was not observed in tumour-bearing mice in the study conducted with [^{68}Ga]Ga-PSMA-11. Roy *et al.* recently performed [^{18}F]DCFPyL

autoradiography/biodistribution study in human, mouse, rat, cynomolgus, and rhesus species and indicated that the binding affinity of [^{18}F]DCFPyL for PSMA was similar across the tested species, although the PSMA expression levels varied. The human submandibular gland exhibited approximately two-fold lower PSMA expression compared with baboons, whereas rodents showed the lowest PSMA levels, with the mouse being 10-fold higher than the rat. Cynomolgus and rhesus monkeys had two- to three-fold lower submandibular gland PSMA levels than humans *(39)*. Different expression patterns of PSMA in human organs compared to its murine homolog, differences in relative binding affinities between [^{68}Ga]Ga-PSMA-11 and [^{18}F]DCFPyL and different pharmacokinetic properties of MSG absorption and clearance between mice and humans may contribute to differences noted between murine and human studies.

All except two lesions were visible on our MSG images; the sample size was not designed to assess the impact of MSG administration on the diagnostic sensitivity for PET imaging. This study aimed at evaluating the potential for MSG to reduce activity retention in the kidneys and salivary glands, with the perspective of eventually using a similar approach for radioligand therapy. The choice of a diagnostic rather than therapeutic radiopharmaceutical was performed for ethical reasons, to avoid compromising a potentially beneficial therapy with an intervention of unknown benefit.

At the oral doses we used in this study, no significant adverse events occurred following the administration of MSG. MSG is a widely studied food additive, with an excellent track record of safety *(40)*. As an orally administered condiment, it would have been an ideal candidate compound for kidney and salivary gland protection due to its low cost, widespread availability, and low toxicity.

Conclusion

In conclusion, our study showed that oral administration of MSG significantly reduced [^{18}F]DCFPyL uptake in salivary glands, kidney and other normal organs in human subjects. However, MSG also caused a corresponding decrease in tumor uptake, which limits the benefits of this approach for use as a means to enhance the therapeutic ratio of PSMA-RLT. Efforts to further improve our understanding of the mechanisms of PSMA radioligands in normal organs may result in more effective preventive and therapeutic strategies. Further investigations are warranted to identify compounds capable of selectively blocking both specific and/or non-specific binding of PSMA radioligands in the salivary glands and the kidneys in order to protect these organs without affecting tumor uptake.

Disclosure

This study was carried out with the financial support of the BC Cancer Foundation, CIHR grant FDN #FDN-148465 and the BC Leadership Chair in Functional Cancer Imaging. The authors report no conflict of interest with the material presented in this study. Dr. François Bénard is co-founder, director and shareholder of Alpha-9 Theranostics, a radiopharmaceutical company.

Key Points

Question

Does orally administered monosodium glutamate (MSG) reduce kidney and salivary gland radiation exposure while using a PSMA targeting radiotracer in human subjects?

Pertinent Findings

In this analysis of a prospective, randomized, double-blind, placebo-controlled intra-individual trial, MSG significantly reduced maximal standardized uptake values corrected for lean body mass in the parotids (24 ± 14%), submandibular glands (35 ± 11%) and kidneys (23 ± 26%) with no adverse events.

Implications for Patient Care

MSG is a candidate compound for kidney and salivary gland protection during PSMA-targeting radioligand therapy.

References

1. Siegel RL, Miller KD, Jemal A. Cancer statistics, 2019. *CA: a cancer journal for clinicians*. 2019;69:7-34.

2. Sharifi N, Dahut WL, Steinberg SM, et al. A retrospective study of the time to clinical endpoints for advanced prostate cancer. *BJU international*. 2005;96:985-989.

3. De Bono JS, Oudard S, Ozguroglu M, et al. Prednisone plus cabazitaxel or mitoxantrone for metastatic castration-resistant prostate cancer progressing after docetaxel treatment: a randomised open-label trial. *The Lancet*. 2010;376:1147-1154.

4. De Bono JS, Logothetis CJ, Molina A, et al. Abiraterone and increased survival in metastatic prostate cancer. *New England Journal of Medicine*. 2011;364:1995-2005.

5. Kantoff PW, Higano CS, Shore ND, et al. Sipuleucel-T immunotherapy for castration-resistant prostate cancer. *New England Journal of Medicine*. 2010;363:411-422.

6. Beer TM, Armstrong AJ, Rathkopf DE, et al. Enzalutamide in metastatic prostate cancer before chemotherapy. *New England Journal of Medicine*. 2014;371:424-433.

7. Parker C, Nilsson S, Heinrich D, et al. Alpha emitter radium-223 and survival in metastatic prostate cancer. *New England Journal of Medicine*. 2013;369:213-223.

8. Pinto JT, Suffoletto BP, Berzin TM, et al. Prostate-specific membrane antigen: a novel folate hydrolase in human prostatic carcinoma cells. *Clinical Cancer Research*. 1996;2:1445-1451.

9. Maurer T, Eiber M, Schwaiger M, Gschwend JE. Current use of PSMA-PET in prostate cancer management. *Nat Rev Urol*. 2016;13:226-235.

10. Rahbar K, Ahmadzadehfar H, Kratochwil C, et al. German Multicenter Study Investigating 177Lu-PSMA-617 Radioligand Therapy in Advanced Prostate Cancer Patients. *J Nucl Med*. 2017;58:85-90.

11. Kratochwil C, Bruchertseifer F, Rathke H, et al. Targeted alpha-Therapy of Metastatic Castration-Resistant Prostate Cancer with (225)Ac-PSMA-617: Dosimetry Estimate and Empiric Dose Finding. *J Nucl Med*. 2017;58:1624-1631.

12. Hofman MS, Violet J, Hicks RJ, et al. [(177)Lu]-PSMA-617 radionuclide treatment in patients with metastatic castration-resistant prostate cancer (LuPSMA trial): a single-centre, single-arm, phase 2 study. *Lancet Oncol*. 2018;19:825-833.

13. Bouchelouche K, Turkbey B, Choyke PL, editors. PSMA PET and radionuclide therapy in prostate cancer. Seminars in nuclear medicine; 2016: Elsevier.

14. von Eyben FE, Roviello G, Kiljunen T, et al. Third-line treatment and 177 Lu-PSMA radioligand therapy of metastatic castration-resistant prostate cancer: a systematic review. *European journal of nuclear medicine and molecular imaging*. 2018;45:496-508.

15. Sarnelli A, Belli ML, Di Iorio V, et al. Dosimetry of 177Lu-PSMA-617 after Mannitol Infusion and Glutamate Tablet Administration: Preliminary Results of EUDRACT/RSO 2016-002732-32 IRST Protocol. *Molecules*. 2019;24:621.

16. Baum RP, Langbein T, Singh A, et al. Injection of botulinum toxin for preventing salivary gland toxicity after PSMA radioligand therapy: an empirical proof of a promising concept. *Nuclear medicine and molecular imaging*. 2018;52:80-81.

17. Rathke H, Kratochwil C, Hohenberger R, et al. Initial clinical experience performing sialendoscopy for salivary gland protection in patients undergoing 225 Ac-PSMA-617 RLT. *European journal of nuclear medicine and molecular imaging*. 2019;46:139-147.

18. Wester H-J, Schottelius M, editors. PSMA-Targeted Radiopharmaceuticals for Imaging and Therapy. Seminars in nuclear medicine; 2019: Elsevier.

19. Matteucci F, Mezzenga E, Caroli P, et al. Reduction of 68 Ga-PSMA renal uptake with mannitol infusion: preliminary results. *European journal of nuclear medicine and molecular imaging*. 2017;44:2189-2194.

20. Jackson PF, Cole DC, Slusher BS, et al. Design, synthesis, and biological activity of a potent inhibitor of the neuropeptidase N-acetylated α-linked acidic dipeptidase. *Journal of medicinal chemistry*. 1996;39:619-622.

21. Chatalic KL, Heskamp S, Konijnenberg M, et al. Towards personalized treatment of prostate cancer: PSMA I&T, a promising prostate-specific membrane antigen-targeted theranostic agent. *Theranostics*. 2016;6:849.

22. Kratochwil C, Giesel FL, Leotta K, et al. PMPA for nephroprotection in PSMA-targeted radionuclide therapy of prostate cancer. *Journal of Nuclear Medicine*. 2015;56:293-298.

23. Majer P, Jančařík A, Krečmerová M, et al. Discovery of orally available prodrugs of the glutamate carboxypeptidase II (GCPII) inhibitor 2-phosphonomethylpentanedioic acid (2-PMPA). *Journal of medicinal chemistry*. 2016;59:2810-2819.

24. Rousseau E, Lau J, Kuo H-T, et al. Monosodium Glutamate Reduces 68Ga-PSMA-11 Uptake in Salivary Glands and Kidneys in a Preclinical Prostate Cancer Model. *Journal of Nuclear Medicine*. 2018;59:1865-1868.

25. Bouvet V, Wuest M, Jans H-S, et al. Automated synthesis of [18 F] DCFPyL via direct radiofluorination and validation in preclinical prostate cancer models. *EJNMMI research*. 2016;6:40.

26. Benjamini Y, Hochberg Y. Controlling the false discovery rate: a practical and powerful approach to multiple testing. *Journal of the Royal statistical society: series B (Methodological)*. 1995;57:289-300.

27. Eiber M, Fendler WP, Rowe SP, et al. Prostate-specific membrane antigen ligands for imaging and therapy. *J Nucl Med*. 2017;58:67S-76S.

28. Virgolini I, Decristoforo C, Haug A, Fanti S, Uprimny C. Current status of theranostics in prostate cancer. *European journal of nuclear medicine and molecular imaging*. 2018;45:471-495.

29. Rousseau E, Wilson D, Lacroix-Poisson F, et al. A prospective study on 18F-DCFPyL PSMA PET/CT imaging in biochemical recurrence of prostate cancer. *Journal of Nuclear Medicine*. 2019;60:1587-1593.

30. Afshar-Oromieh A, Babich JW, Kratochwil C, et al. The rise of PSMA ligands for diagnosis and therapy of prostate cancer. *Journal of Nuclear Medicine*. 2016;57:79S-89S.

31. Ristau BT, O'Keefe DS, Bacich DJ, editors. The prostate-specific membrane antigen: lessons and current clinical implications from 20 years of research. Urologic Oncology: Seminars and Original Investigations; 2014: Elsevier.

32. Holland JP, Divilov V, Bander NH, Smith-Jones PM, Larson SM, Lewis JS. 89Zr-DFO-J591 for immunoPET of prostate-specific membrane antigen expression in vivo. *J Nucl Med*. 2010;51:1293-1300.

33. Silver DA, Pellicer I, Fair WR, Heston WD, Cordon-Cardo C. Prostate-specific membrane antigen expression in normal and malignant human tissues. *Clin Cancer Res*. 1997;3:81-85.

34. Kratochwil C, Bruchertseifer F, Rathke H, et al. Targeted α-therapy of metastatic castration-resistant prostate cancer with 225Ac-PSMA-617: swimmer-plot analysis suggests efficacy regarding duration of tumor control. *Journal of Nuclear Medicine*. 2018;59:795-802.

35. Valkema R, Pauwels SA, Kvols LK, Kwekkeboom DJ. Long-Term Follow-Up of Renal Function After Peptide Receptor Radiation Therapy with^ sup 90^ Y-DOTA^ sup 0^, Tyr^ sup 3^-Octreotide and^ sup 177^ Lu-DOTA^ sup 0^, Tyr^ sup 3^-Octreotate. *The Journal of Nuclear Medicine*. 2005;46:83S.

36. von Eyben FE, Baumann GS, Baum RP. PSMA diagnostics and treatments of prostate cancer become mature. *Clinical and translational imaging*. 2018;6:145-148.

37. Hillier SM, Maresca KP, Femia FJ, et al. Preclinical evaluation of novel glutamate-urea-lysine analogues that target prostate-specific membrane antigen as molecular imaging pharmaceuticals for prostate cancer. *Cancer research*. 2009;69:6932-6940.

38. Nedelcovych MT, Dash RP, Wu Y, et al. JHU-2545 Selectively Shields Salivary Glands and Kidneys during PSMA-Targeted Radiotherapy. *bioRxiv*. 2019457085.

39. Roy J, Warner BM, Basuli F, et al. Comparison of Prostate-Specific Membrane Antigen Expression Levels in Human Salivary Glands to Non-Human Primates and Rodents. *Cancer Biotherapy & Radiopharmaceuticals*. 2020.

40. Mortensen A, Aguilar F, Crebelli R, et al. Re-evaluation of glutamic acid (E 620), sodium glutamate (E 621), potassium glutamate (E 622), calcium glutamate (E 623), ammonium glutamate (E 624) and magnesium glutamate (E 625) as food additives. *EFSA Journal*. 2017;15:e04910.

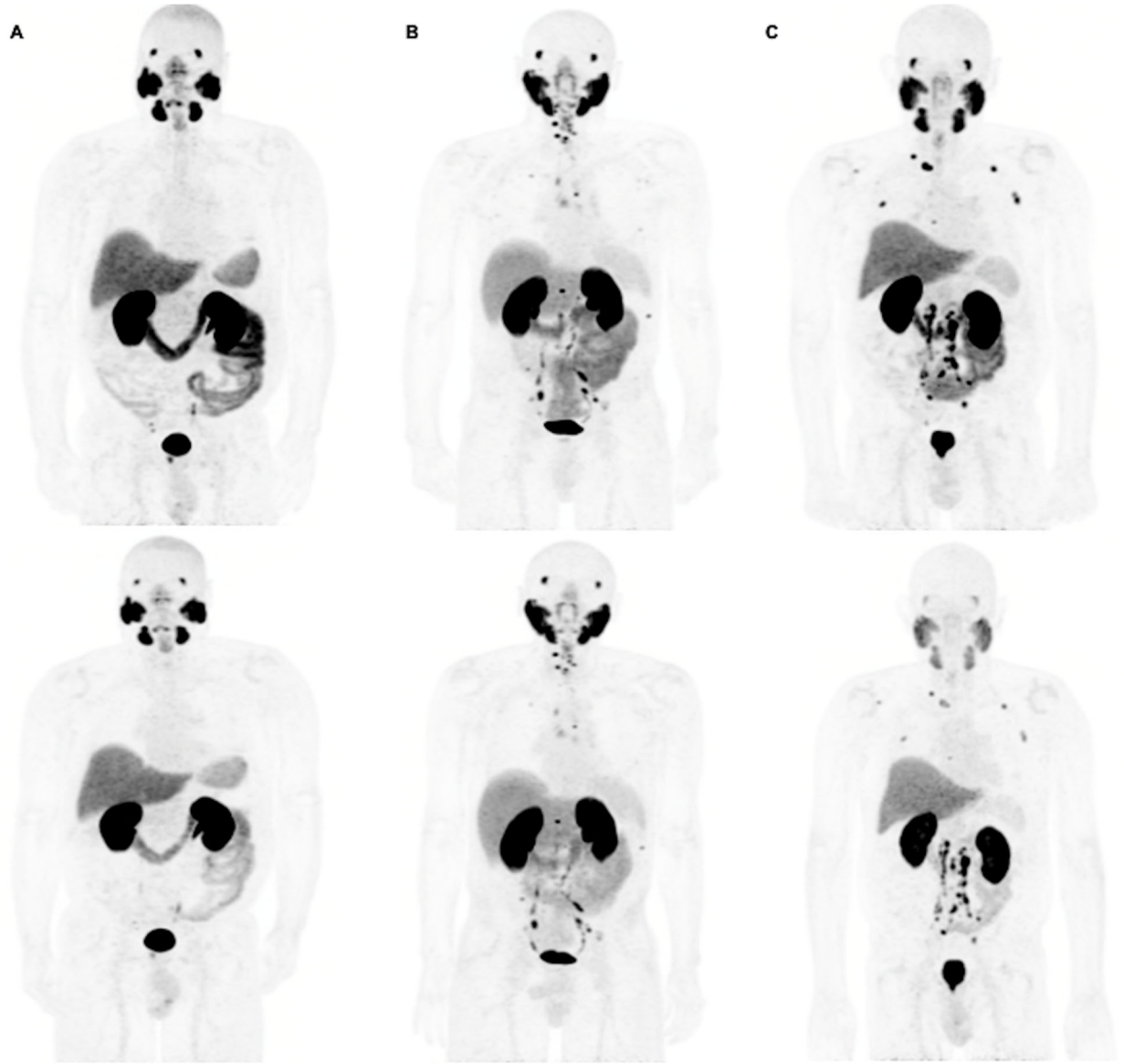

Figure 1. Representative anterior maximum intensity projections (MIPs) of patients 2 (A), 4 (B), and 10 (C) with the placebo images in the upper row and the MSG images in the bottom row.

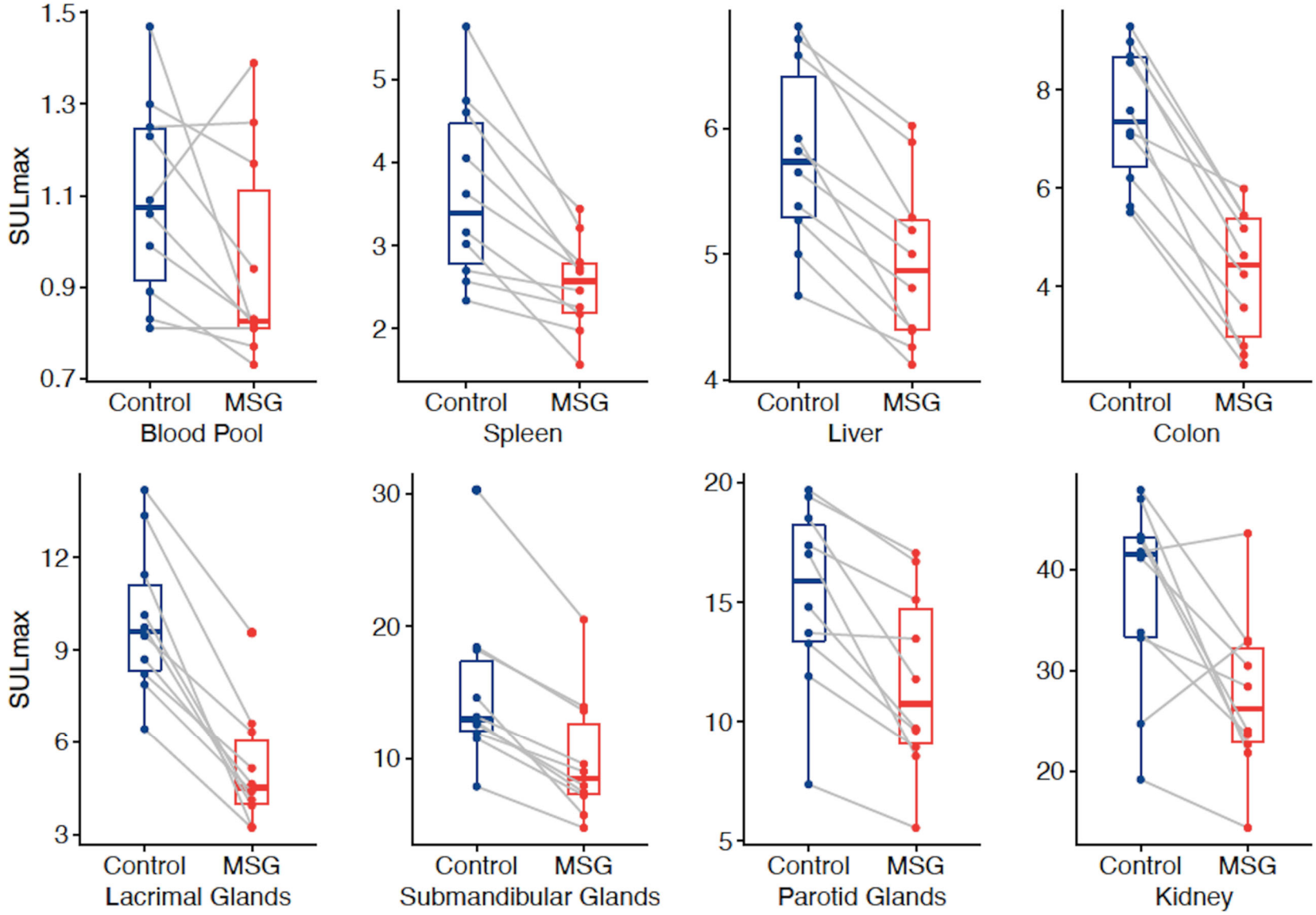

Figure 2. SULmax of normal tissues in control and MSG PET/CT studies.

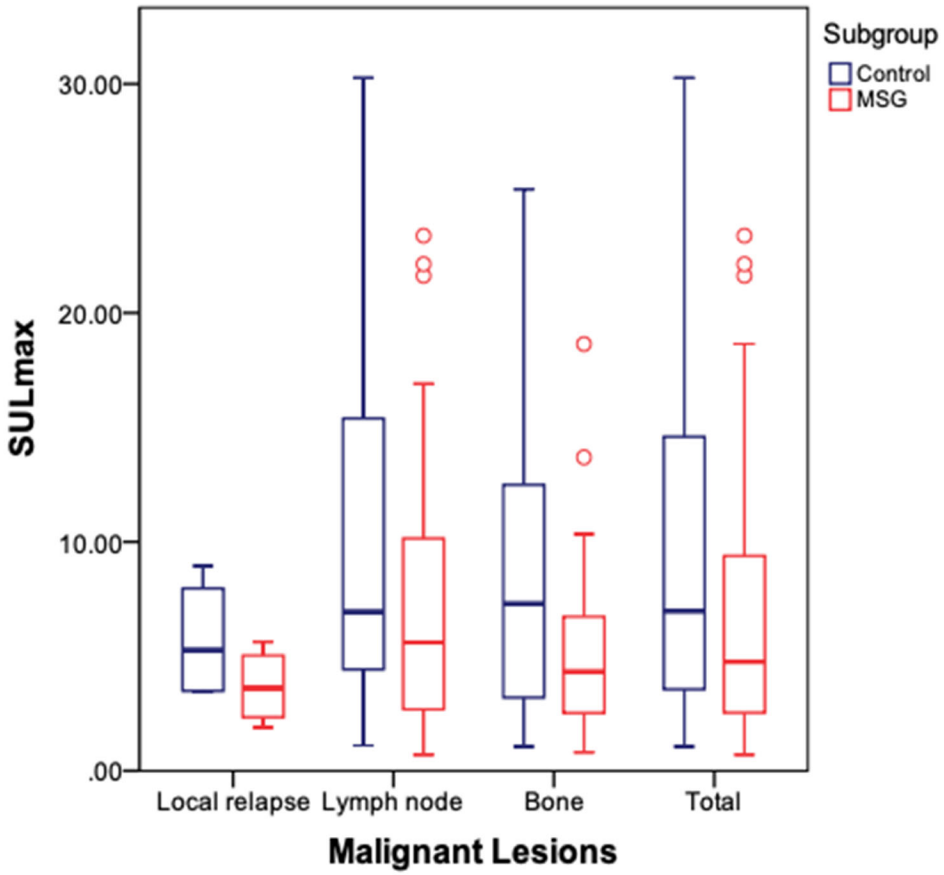

Figure 3. Comparison of SULmax values of local relapses, lymph node metastases, osseous metastases, and total malignant lesions provided by the control and MSG PET/CT studies.

Table 1. Patients characteristics.

Patient	Age (years)	Weight (kg)	Height (cm)	TNM	Gleason score	Previous therapy	PSA value (ng/mL)	PSA doubling time (months)	MSG dose (mg/kg)	Injected activity (MBq)		Uptake time (min)
										Control study	MSG study	
1	73	72.3	160	pT3apN0M0	7 (3+4)	RP+RT+ADT	3.3	39.2	175.66	289.9	316.1	120
2	72	86.2	170	cT2acN0M0	7 (4+3)	RT	2.13	9.9	147.33	344.8	366.8	120
3	69	85.3	173	cT2ccN0M0	8	RT	4.67	3	148.89	366.2	339	120
4	62	76.6	181	cT2bcN0M0	7 (3+4)	RT	30	23.7	165.79	369.1	388.12	120
5	75	77.6	169	pT3apN0M0	7 (4+3)	RP	0.62	-	163.66	353	382.7	120
6	71	110.2	180	cT2cN0M0	7 (3+4)	RT+ADT	6.5	5.3	115.24	410.1	410.1	120
7	69	93	183	pT3bpN0M0	7 (4+3)	RP+RT	0.93	3.2	136.56	354.2	359.2	120
8	76	92.3	172.5	pT3apN0M0	7 (4+3)	RP+RT	0.92	6.7	137.59	340.9	360.8	120
9	76	92.1	180	pT3apN0M0	7 (4+3)	RP+RT+ADT	0.44	6.5	137.89	373	348.6	120
10	77	77.1	170	pT3bpN1M0	7 (3+4)	RP+RT	16.7	4.2	164.72	354	329.7	120

RP, radical prostatectomy; RT, radiotherapy; ADT, androgen deprivation therapy; PSA, prostate specific antigen; MSG, monosodium glutamate

Table 2. Comparison of [^{18}F]DCFPyl uptake in normal tissues in control and MSG studies.

Tissue	Average SULmean				Average SULmax			
	Control (N=10)	**MSG (N=10)**	**Percentage decrease (%) (N=10)**	**Adj. *P* value$^{\Psi}$**	**Control (N=10)**	**MSG (N=10)**	**Percentage decrease (%) (N=10)**	**Adj. *P* value$^{\Psi}$**
Blood pool	**0.8 ± 0.1**	**0.7 ± 0.1**	**10.7 ± 12.5**	**0.021**	1.1 ± 0.2	0.9 ± 0.2	11.4 ± 19.1	0.081
Gluteus muscle	0.2 ± 0.05	0.2 ± 0.04	7.9 ± 21.7	0.100	0.3 ± 0.1	0.3 ± 0.1	2.7 ± 27.9	0.364
Liver	**4.5 ± 0.6**	**3.7 ± 0.6**	**15.7 ± 7.3**	**<0.001**	**5.8 ± 0.7**	**4.9 ± 0.7**	**14.6 ± 5.7**	**<0.001**
Spleen	**3.2 ± 0.9**	**2.1 ± 0.6**	**34.3 ± 11.1**	**<0.001**	**3.6 ± 1.1**	**2.5 ± 0.6**	**28.3 ± 13.4**	**0.001**
Parotid glands	**9.1 ± 2.5**	**6.9 ± 2.9**	**26.1 ± 16.9**	**0.003**	**15.3 ± 3.9**	**11.6 ± 3.8**	**23.9 ± 14.0**	**0.001**
Submandibular glands	**8.9 ± 3.5**	**5.8 ± 2.9**	**34.7 ± 18.7**	**0.001**	**15.1 ± 6.2**	**9.9 ± 4.8**	**35.0 ± 11.2**	**<0.001**
Lacrimal glands	**6.0 ± 1.3**	**3.4 ± 1.2**	**41.9 ± 18.9**	**<0.001**	**9.9 ± 3.4**	**5.1 ± 1.9**	**48.5 ± 12.5**	**<0.001**
Colon	**5.9 ± 1.2**	**3.3 ± 1.2**	**45.1 ± 13.8**	**<0.001**	**7.5 ± 1.4**	**4.2 ± 1.3**	**43.8 ± 12.9**	**<0.001**
Urinary bladder	33.8 ± 9.9	27.9 ± 10.2	14.8 ± 30.2	0.054	73.0 ± 29.3	63.5 ± 33.8	14.4 ± 32.5	0.124
Kidneys	**17.2 ± 4.6**	**12.1 ± 2.2**	**27.4 ± 12.1**	**0.001**	**37.5 ± 9.6**	**27.4 ± 8.0**	**23.5 ± 26.1**	**0.012**

The bold values indicate statistical significance at the $\alpha = 0.05$ level.

Ψ Adjusted P-value for multiple testing using Benjamini–Hochberg method.

Table 3. Comparison of [^{18}F]DCFPyl uptake in malignant lesions for the control and MSG studies.

Parameter	Control study (N=142)	MSG study (N=140)	Percentage decrease (%)	*P* value
Median [range] SULmax	**4.4 [1.1, 30.3]**	**2.8 [0.7, 23.4]**	**32.8 [-1.3, 74.5]**	**<0.001**
Median [range] SULmean	**2.9 [0.9, 17.1)**	**1.6 [0.6, 14.5]**	**29.1 [0.0, 73.5]**	**<0.001**
Median [range] SULpeak	**4.1 [0.7, 21.1]**	**3.0 [0.5, 16.8]**	**30.1 [-46.6, 71.6]**	**<0.001**

The bold values indicate statistical significance at the $\alpha = 0.05$ level.

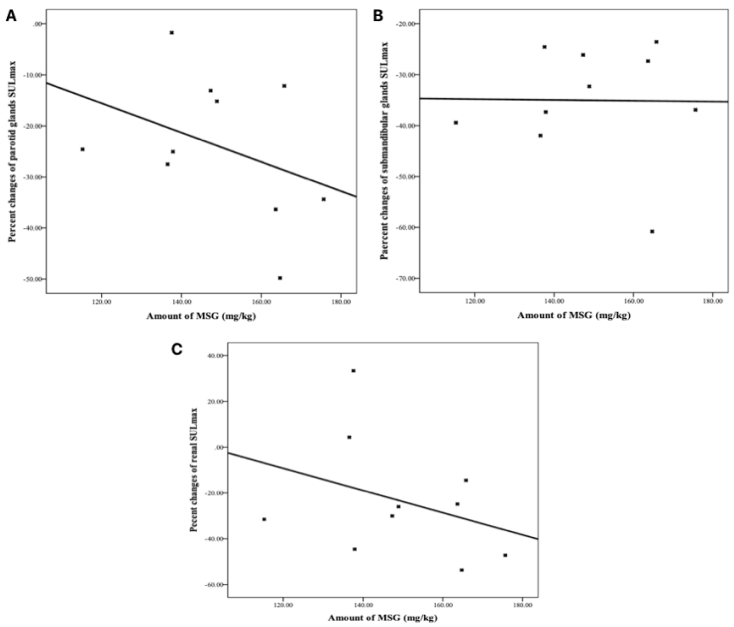

Supplemental Figure 1. Dose-response relationship between the MSG amount normalized to body weight and percentage changes of parotid glands (A), submandibular glands (B) and renal (C) SULmax.